

Synthesis of two tantalum complexes bearing cyclopentadienyl analogs

Caroline K. Sperry, George Rodriguez, Guillermo C. Bazan *

Department of Chemistry, University of Rochester, Rochester, NY 14627, USA

Received 3 October 1996; received in revised form 13 December 1996

Abstract

Reaction of $\text{Li}[\text{C}_5\text{H}_5\text{B-NMe}_2]$ with (TBM) TaMe_2Cl (TBM = tribenzylidenemethane) gives (TBM) $[\text{C}_5\text{H}_5\text{B-NMe}_2]\text{TaMe}_2$ (**1**). A single crystal diffraction study revealed a metallocene-like environment with the metal binding more strongly to the boratabenzene ring carbons furthest from the boron atom. $\text{Cp}^*[\text{C}_4\text{H}_4\text{B-N(CHMe}_2)_2]\text{Ta}(\eta^1\text{-C}_4\text{H}_6)$ (**2**) ($\text{Cp}^* = \text{C}_5\text{Me}_5$) is obtained from the reaction of $\text{Cp}^*[\text{C}_4\text{H}_4\text{B-N(CHMe}_2)_2]\text{TaCl}_2$ and $(\text{C}_4\text{H}_6\text{Mg})(\text{THF})_2$. The diene fragment binds in a trans configuration. The oxidation state of tantalum in **2** can be considered as I, III or V if all resonance contributions are taken into account. © 1997 Elsevier Science B.V.

1. Introduction

There is a significant and growing interest in seeking new ligands that behave similarly to cyclopentadienyl for synthesizing group 4 metallocene-like compounds (for a recent overview see [1]). This drive is fuelled, in part, by the potential of building unique catalysts for the polymerization of olefins. New catalysts may ultimately lead to polymers with novel structures which in turn may be of commercial importance. Recent progress in the chemistry of electrophilic metallocenes, of both d^0 transition metals and lanthanides, has also made an impact in diverse areas of chemical research. These areas include the development of organic reactions, catalytic reactions, such as hydrosilylation [2] and hydroamination [3], C-H activation processes, and the polymerization of silanes [4] and stannanes [5]. The search for new metallocene environments is therefore likely to have an influence on many branches of chemistry.

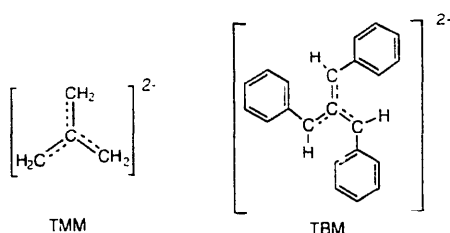
Early synthetic, structural, and mechanistic studies focused on the dianionic dicarbollide ligand, $(\text{C}_2\text{B}_9\text{H}_{11})^{2-}$. By replacing a cyclopentadienyl ligand with $[\text{C}_2\text{B}_9\text{H}_{11}]^{2-}$ the charge of the complex increases by one negative unit while the overall molecular geom-

try and frontier orbitals remain relatively unperturbed [6]. Complexes with general formula $\text{Cp}^*[\text{C}_2\text{B}_9\text{H}_{11}]\text{MMe}(\text{THF})$ ($\text{Cp}^* = \text{C}_5\text{Me}_5$, M = Hf, Zr) were the first high valent compounds to be reported [7] and displayed chemistry similar to that of group 3 bis-cyclopentadienyl complexes such as Cp_2^*ScMe [8]. The synthesis of $(\text{Cp}^*[\text{C}_2\text{B}_9\text{H}_{11}]\text{ScCH}(\text{SiMe}_3)_2)^-(\text{Li}(\text{THF}))^+$ and $(\text{C}_5\text{H}_4\text{CH}_3)[\text{C}_2\text{B}_9\text{H}_{11}]\text{TaMe}_2$ continued this line of research [9,10]. For the scandium complex, the hydridic B-H functionalities proved to be effective bases which prevented olefin insertion. Similarly, strong coordination to Zr was observed for $\text{Cp}^*[\text{C}_2\text{B}_9\text{H}_{11}]\text{ZrMe}$ derivatives. Activation of the Ta-C bond to generate reactive cationic species was not reported in the case of $(\text{C}_5\text{H}_4\text{CH}_3)[\text{C}_2\text{B}_9\text{H}_{11}]\text{TaMe}_2$ [10]. These problems, and in particular the propensity of boron hydrides to bind tightly to electrophilic metal centers, prompted the search for 6 π electron ligands which do not contain basic functionalities (for recent advances in the chemistry of related carborane metal complexes see [11]).

The trimethylenemethane (TMM) fragment is formally a dianionic 6 π electron donor which has found extensive use in low valent transition metal chemistry [12]. The related fragment, tribenzylidenemethane (TBM), contains three phenyl rings on the periphery of the TMM framework and was used in the preparation of $[\text{Cp}^*(\text{TBM})\text{ZrCl}_2][\text{Li}(\text{TMEDA})_2]$ [13] (TMEDA =

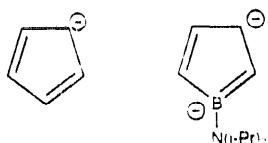
* Corresponding author.

N,N,N',N'-tetramethylethylenediamine) and Cp*(TBM)TaMe₂ [14]:



Ethylene polymerization is possible by activation of [Cp*(TBM)ZrCl₂][Li(TMEDA)₂] with methylaluminoxane (MAO). The reactive species is most likely neutral Cp*(TBM)ZrMe [15]. Attempts to activate Cp*(TBM)TaMe₂, and related complexes, using acids or oxidants have thus far failed to give well defined catalysts. Only when MAO is added to Cp*(TBM)TaMe₂ are polymerization activities observed, but catalyst lifetime is short [16].

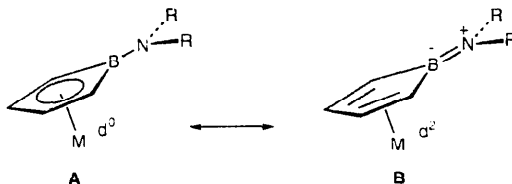
Complexes containing borollide heterocycles were also prepared within the context of polymerization chemistry. Borollide ligands are close structural relatives of Cp (Cp = C₅H₅) (for a recent review of borollide chemistry see [17]). The dianionic charge in these molecular fragments is readily understood in terms of an isoelectronic boron anion for neutral carbon atom substitution in the five-membered aromatic ring:



In [Cp*[C₄H₄B-N(CHMe₂)₂]MCl₂Li(OEt₂)₂] (M = Zr, Hf) the metal center, in conjunction with the basic amine, were shown to participate in heterolytic bond activation reactions; however, their reactivity toward olefins remains unreported [18]. The tantalum complex Cp*[η⁵-C₄H₄B-N(CHMe₂)₂]TaMe₂ is similar in structure to Cp₂*ZrMe₂ and displays similar isocyanide insertion and metal–alkyl hydrogenation chemistry [19]. Polymerization activity with MAO, however, is well below those reported for standard group 4 metallocenes.

In borollide complexes the orbital overlap between boron and the metal depends on the π donating ability of the boron substituent. Nitrogen containing functionalities participate in strong B = N π orbital overlap and weaken the metal–boron interaction (this effect obeys the series N > O > P > other substituents on boron). These interactions weaken the boron–metal bond and

make the ligands similar to dienes. (For a detailed discussion see [20].) Structural characterization of aminoborollide metallocenes consistently show long metal–boron distances and short B–N bond lengths (in the order of 1.40 Å). These complexes are thus ‘ambivalent’, requiring resonance contributions A and B to account for their metrical parameters:



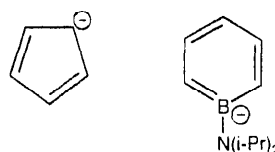
Eliminating the boron-exocyclic π interaction, either by protonation of the amine or by using a methyl substituent, contracts the boron–metal distances and favors the high oxidation state description A. Therefore, it is possible to control the electron density at the metal center using boron heterocycles in a way not readily achievable with cyclopentadienyl ligands.

Relevant to the discussion here are diene complexes of general composition Cp*(η^4 -diene)MCl₂ (M = Nb and Ta) [21]. In the presence of MAO, these serve as catalyst precursors for the living polymerization of ethylene [22]. These complexes are usually viewed as d⁰, 14 electron complexes in which the diene fragment is formally dianionic. It is important to recall that dienes have two resonance forms:



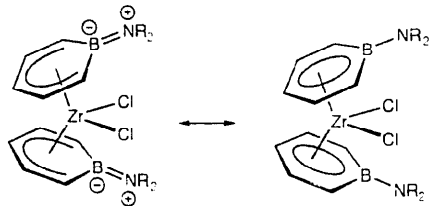
Late transition metal complexes are usually described as π -complexes, while the early transition metal counterparts have bond distances more consistent with metallacyclopentene binding [23].

Boratabenzene rings were used for the synthesis of [C₅H₅B-N(CHMe₂)₂]₂ZrCl₂ [24]. This boracycle may be viewed as the six-membered analog of the Cp ligand and has found extensive use in the preparation of low valent complexes [25]:



In [C₅H₅B-N(CHMe₂)₂]₂ZrCl₂ a strong B = N π interaction exists and boratabenzene binds in a pentadi-

enyl-like fashion with boron projected away from the metal. This distortion allows for zirconium to interact more strongly with the electron-rich carbons opposite to boron. Boratabenzene metallocenes are excellent precursors for olefin polymerization catalysts and hold the promise of controlling the reactivity by choice of exocyclic substituent [23]:

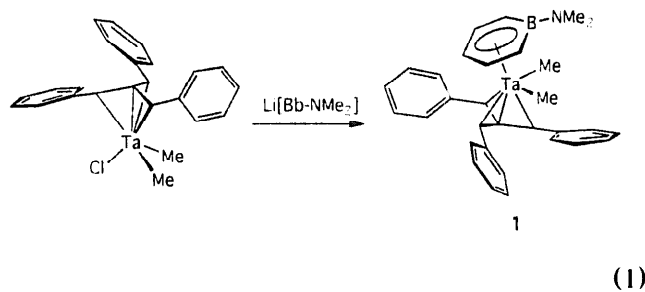


In this contribution we report the synthesis and structural characterization of $(TBM)[C_5H_5B-N(Me)_2]TaMe_2$ (**1**) and $Cp^*[\eta^5-C_4H_4B-NMe_2]Ta(\eta^5-C_4H_6)$ (**2**). These complexes combine dianionic ligands and boron heterocycles within the coordination sphere of tantalum. Their structural characterization provides insight into metal–ligand bonding interactions.

2. Results and discussion

2.1. $(TBM)[C_5H_5B-NMe_2]TaMe_2$

Addition of $Li[C_5H_5B-NMe_2]$ ($Li[Bb-NMe_2]$) to 1 equiv of $(TBM)TaMe_2Cl$ in tetrahydrofuran followed by toluene extraction gives $(TBM)[Bb-NMe_2]TaMe_2$ (**1**) in 60% isolated yield:



Single crystals suitable for X-ray crystallography were grown from a concentrated diethyl ether solution. The results of this study are shown in Fig. 1 and Tables 1–4. The overall molecular arrangement of **1** is similar to that of a group 4 metallocene with TBM and $Bb-NMe_2$ occupying the pseudotetrahedral cyclopentadienyl sites. Note that the angle defined by $C_1-Ta-[Bb-NMe_2]_{\text{centroid}}$

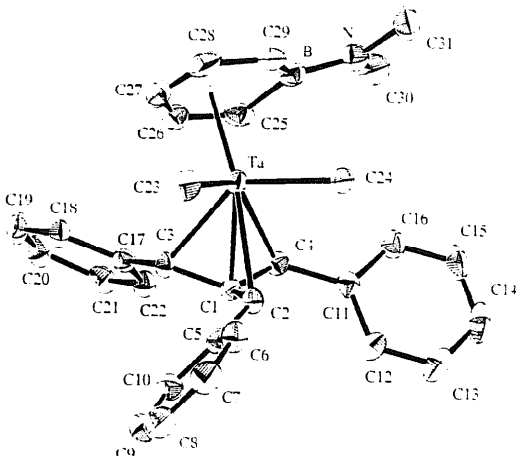


Fig. 1. ORTEP drawing of **1** at 50% probability. Hydrogen atoms are omitted for clarity.

Table 1
Crystal, data collection and refinement parameters of **1**

Empirical formula	TaC ₃₂ H ₄₅ BN
Formula weight (amu)	623.46
Crystal size (mm)	0.20 × 0.15 × 0.20
Color	ruby-red
Cryst syst	triclinic
Lattice type	Primitive
Space group	P $\bar{1}$ (#2)
Z	2
a (Å)	8.4248(1)
b (Å)	12.2310(0)
c (Å)	12.6993(1)
V (Å ³)	1282.17(2)
α°	93.982(1)
β°	99.136(1)
γ°	95.121(1)
d _{calc} (g/cm ³)	1.62
T (°C)	-60
Diffractometer	Siemens-SMART
$\lambda_{Mo K\alpha}$ (graphic monochromated radiation)	0.71069
Scan rate (deg/min)	1.8
No. frames	1321
Time to acquire frames (sec/frame)	10
No. of unique reflections collected	Total: 8187 Unique: 5764 ($R_{\text{int}} = 0.027$)
No. of observations ($I > 3.00(I)\sigma$)	5299
No. of parameters varied	307
abs. coeff. cm ⁻¹	43.1
Range of transm factors	0.44225–0.78408
R ₁ ^a	0.032
R ₂ ^b	0.068
Max. Shift/error in final cycle	0.04
Goodness of fit ^c	3.41
Max. peak	0.81
min peak	−1.48

^a $R_1 = \sum(|F_o| - |F_c|)/\sum|F_o|$. ^b $R_2 = [\sum w(|F_o| - |F_c|)^2 / \sum w|F_o|^2]^{1/2}$.

^cS = goodness of fit = $(\sum(|F_o| - |F_c|)/\sigma)/(n-m)$, where n is the number of reflections used in the refinement and m is the number of variables.

Table 2
Atomic coordinates and B_{eq} for 1

Atom	x	y	z	B_{eq}
Ta	0.07324(4)	0.28419(2)	0.18209(2)	1.673(7)
N	0.3339(9)	0.5138(6)	0.3962(6)	2.5(1)
C(1)	-0.2012(8)	0.2789(6)	0.1617(6)	1.7(1)
C(2)	-0.1786(9)	0.2941(6)	0.0541(6)	1.8(1)
C(3)	-0.1682(9)	0.1715(6)	0.1970(6)	1.8(1)
C(4)	-0.1564(9)	0.3705(6)	0.2396(6)	1.7(1)
C(5)	-0.2500(9)	0.2176(6)	-0.0412(6)	1.9(1)
C(6)	-0.192(1)	0.2267(7)	-0.1397(6)	2.6(2)
C(7)	-0.266(1)	0.1626(8)	-0.2330(7)	3.3(2)
C(8)	-0.396(1)	0.0889(8)	-0.2316(7)	3.3(2)
C(9)	-0.457(1)	0.0769(8)	-0.1368(8)	3.3(2)
C(10)	-0.383(1)	0.1406(7)	-0.0415(7)	2.7(2)
C(11)	-0.1871(9)	0.4862(6)	0.2225(6)	2.0(1)
C(12)	-0.309(1)	0.5155(7)	0.1434(7)	2.5(2)
C(13)	-0.341(1)	0.6237(8)	0.1378(8)	3.3(2)
C(14)	-0.251(1)	0.7060(8)	0.2105(9)	3.7(2)
C(15)	-0.132(1)	0.6777(7)	0.2879(9)	3.5(2)
C(16)	-0.101(1)	0.5704(7)	0.2930(7)	2.6(2)
C(17)	-0.2089(9)	0.1230(6)	0.2948(6)	1.8(1)
C(18)	-0.162(1)	0.0186(7)	0.3160(7)	2.3(2)
C(19)	-0.196(1)	-0.0311(7)	0.4043(7)	2.8(2)
C(20)	-0.281(1)	0.0203(7)	0.4743(7)	2.9(2)
C(21)	-0.333(1)	0.1218(7)	0.4543(7)	2.5(2)
C(22)	-0.2967(10)	0.1731(6)	0.3654(6)	2.0(2)
C(23)	0.111(1)	0.1702(8)	0.0472(7)	3.0(2)
C(24)	0.1275(10)	0.4478(7)	0.1255(7)	2.5(2)
C(25)	0.1611(10)	0.3246(8)	0.3866(6)	2.5(2)
C(26)	0.150(1)	0.2125(8)	0.3617(7)	3.1(2)
C(27)	0.238(1)	0.1665(8)	0.2881(9)	3.8(2)
C(28)	0.347(1)	0.2326(8)	0.2433(8)	3.4(2)
C(29)	0.3672(10)	0.3484(7)	0.2640(7)	2.5(2)
C(30)	0.268(1)	0.5631(8)	0.4846(8)	3.5(2)
C(31)	0.452(1)	0.5899(8)	0.3621(8)	3.5(2)
B	0.293(1)	0.4045(8)	0.3544(7)	2.3(2)

Table 3
Bond distances (\AA) of 1

Atom	Atom	Distance (\AA)	Atom	Atom	Distance (\AA)
Ta	C(1)	2.280(7)	C(6)	C(7)	1.40(1)
Ta	C(2)	2.477(7)	C(7)	C(8)	1.36(1)
Ta	C(3)	2.394(8)	C(8)	C(9)	1.39(1)
Ta	C(4)	2.469(7)	C(9)	C(10)	1.42(1)
Ta	C(23)	2.212(8)	C(11)	C(12)	1.41(1)
Ta	C(24)	2.207(8)	C(11)	C(16)	1.39(1)
Ta	C(25)	2.585(8)	C(12)	C(13)	1.38(1)
Ta	C(26)	2.509(8)	C(13)	C(14)	1.40(2)
Ta	C(27)	2.419(9)	C(14)	C(15)	1.38(2)
Ta	C(28)	2.467(8)	C(15)	C(16)	1.36(1)
Ta	C(29)	2.560(8)	C(17)	C(18)	1.40(1)
N	C(30)	1.45(1)	C(17)	C(22)	1.39(1)
N	C(31)	1.44(1)	C(18)	C(19)	1.37(1)
N	B	1.40(1)	C(19)	C(20)	1.38(1)
C(1)	C(2)	1.43(1)	C(20)	C(21)	1.38(1)
C(1)	C(3)	1.45(1)	C(21)	C(22)	1.39(1)
C(1)	C(4)	1.42(1)	C(25)	C(26)	1.38(1)
C(2)	C(5)	1.49(1)	C(25)	B	1.54(1)
C(3)	C(17)	1.49(1)	C(26)	C(27)	1.40(2)
C(4)	C(11)	1.49(1)	C(27)	C(28)	1.38(2)
C(5)	C(6)	1.42(1)	C(28)	C(29)	1.41(1)
C(5)	C(10)	1.39(1)	C(29)	B	1.54(1)

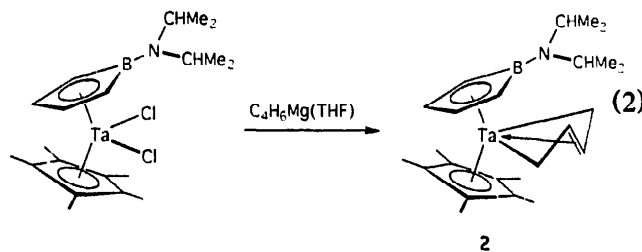
Table 4
Selected bond angles ($^\circ$) for 1

Atom	Atom	Atom	Angle	Atom	Atom	Atom	Angle
C(23)	Ta	C(24)	102.8(4)				
C(30)	N	C(31)	111.2(8)	C(30)	N	B	123.7(8)
C(31)	N	B	125.1(8)	C(2)	C(1)	C(3)	114.7(6)
C(2)	C(1)	C(4)	117.8(7)	C(3)	C(1)	C(4)	116.5(6)
C(26)	C(27)	C(28)	120.6(9)	C(27)	C(28)	C(29)	122.1(9)
C(28)	C(29)	B	120.6(8)	N	B	C(25)	125.3(8)
N	B	C(29)	124.7(8)	C(25)	B	C(29)	110.0(8)

(133.7(8) $^\circ$) matches with the $\text{Cp}^*_\text{centroid}-\text{Zr}-\text{Cp}^*_\text{centroid}$ angle (132.5 $^\circ$) of $\text{Cp}_2^*\text{ZrMe}_2$ [26]. Disruption of boratabenzene aromaticity is suggested by the long Ta–B (2.82(2) \AA) and short B–N (1.40(1) \AA) distances, which are typical distortions in boron heterocycles ligated to high valent early transition metals. Tantalum binds progressively more tightly to the ring carbons furthest away from boron (in \AA : Ta–C₂₉ = 2.560(8), Ta–C₂₈ = 2.467(8), Ta–C₂₇ = 2.418(9)). Thus, as in $[\text{C}_5\text{H}_5\text{B}(\text{CHMe}_2)_2]_2\text{ZrCl}_2$, there is significant η^5 -pentadienyl character in the boratabenzene ligand.

2.2. $\text{Cp}^*[\text{C}_4\text{H}_4\text{BN}(\text{CHMe}_2)_2]\text{Ta}(\eta^4\text{-C}_4\text{H}_6)$

Reaction in THF of $(\text{C}_4\text{H}_6\text{Mg})(\text{THF})_2$ with $\text{Cp}^*[\text{C}_4\text{H}_4\text{B}(\text{N}(\text{CHMe}_2)_2)]\text{TaCl}_2$ gives $\text{Cp}^*[\text{C}_4\text{H}_4\text{B}(\text{N}(\text{CHMe}_2)_2)]\text{Ta}(\text{trans-}\eta^4\text{-C}_4\text{H}_6)$ (2) in approximately 70% yield, as shown in:



Determination of hapticity and stereochemistry for the diene fragment was not straightforward using solution spectroscopy and required solid state characterization. Table 5 gives relevant crystal and data collection parameters. Atomic coordinates are given in Table 6 with important intramolecular distances and angles in Tables 7 and 8. As shown in Fig. 2, all four carbons of the diene are firmly bound to tantalum (Ta–C₂₄ = 2.39(1) \AA ; Ta–C₂₃ = 2.344(10) \AA ; Ta–C₂₂ = 2.293(10) \AA ; Ta–C₂₁ = 2.45(1) \AA) and have equidistant C–C bonds (C₂₄–C₂₃ = 1.42(2) \AA ; C₂₃–C₂₂ = 1.45(1) \AA ; C₂₁–C₂₂ = 1.44(2) \AA [27]). The borollide–Ta interaction conforms to the usual ambivalent situation (Ta–B = 2.73(1) \AA ; B–N = 1.42(1) \AA , sp² hybridized N). Therefore, the

Table 5
Crystal, data collection and refinement parameters of **2**

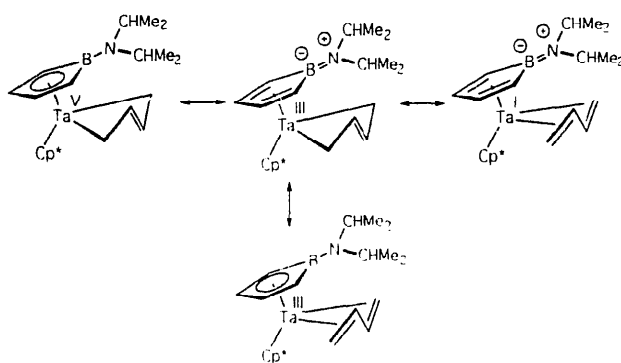
Empirical formula	C ₂₄ H ₃₇ BNTa
Formula weight (amu)	531.32
Crystal size (mm)	0.08 × 0.02 × 0.08
Color	yellow
Cryst syst	monoclinic
Lattice type	Primitive
Space group	P2 ₁ /c(#14)
Z	4
a (Å)	13.628(1)
b (Å)	17.889(2)
c (Å)	17.889(2)
β°	103.130(1)
V (Å ³)	2266.5(3)
d _{calc} (g/cm ³)	1.56
T (°C)	-50
Diffractometer	Siemens-SMART
λ _{Mn} K _α (graphite monochromated radiation)	0.71069
Scan rate (deg/min)	1.8
2θ range (deg)	0–50
Data collected	h, k, ± l
No. of reflections measured	Total: 13445 Unique: 5551 ($R_{\text{int}} = 0.090$)
No. of observations (I > 3.00(I)σ)	2511
No. of parameters varied	244
abs. coeff (cm ⁻¹)	39.1
abs. correction	empirical
Range of transm factors	0.15012–0.32388
R ₁ ^a	0.051
R ₂ ^b	0.038
Max. Shift/error in final cycle	0.03
Goodness of fit ^c	1.54
Max. peak	1.00
Min. peak	-1.05

^a R₁ = $\sum(|F_o| - |F_c|)/\sum|F_o|$.

^b R₂ = $[\sum w(|F_o| - |F_c|)^2 / \sum w|F_o|^2]^{1/2}$.

^c S = goodness of fit = $(\sum(|F_o| - |F_c|)/\sigma)/(n-m)$, where n is the number of reflections used in the refinement and m is the number of variables.

different resonance contributions allow for consideration of oxidation states I, III and V:



The ¹H NMR spectrum of **2** shows four signals for the borollide ring and six for the butadiene ligand. These

Table 6
Atomic coordinates and B_{eq} for **2**

Atom	x	y	z	B _{eq}
Ta(1)	0.19014(3)	0.16387(5)	0.37322(3)	2.312(8)
N(1)	0.2893(6)	-0.0450(8)	0.2190(5)	2.2(2)
C(1)	0.2918(7)	0.363(1)	0.4352(6)	2.3(2)
C(2)	0.1896(8)	0.387(1)	0.4390(6)	2.5(3)
C(3)	0.1615(8)	0.287(1)	0.4875(6)	2.7(3)
C(4)	0.2450(8)	0.196(1)	0.5143(6)	2.8(3)
C(5)	0.3229(8)	0.241(1)	0.4796(6)	2.5(3)
C(6)	0.3578(9)	0.458(1)	0.4054(7)	4.3(3)
C(7)	0.1272(9)	0.512(1)	0.4061(7)	4.4(3)
C(8)	0.0692(9)	0.289(1)	0.5195(7)	5.2(4)
C(9)	0.2532(9)	0.094(1)	0.5784(7)	4.3(3)
C(10)	0.4290(8)	0.186(1)	0.4966(7)	4.1(3)
C(11)	0.1279(8)	0.096(1)	0.2396(6)	3.1(3)
C(12)	0.1100(10)	0.241(1)	0.2510(6)	3.6(3)
C(13)	0.1999(9)	0.311(1)	0.2735(6)	3.3(3)
C(14)	0.2809(8)	0.215(1)	0.2771(6)	2.9(3)
C(15)	0.3957(8)	-0.040(1)	0.2142(6)	3.2(3)
C(16)	0.2315(8)	-0.165(1)	0.1809(6)	3.5(3)
C(17)	0.4684(8)	-0.034(1)	0.2925(7)	4.9(3)
C(18)	0.4166(9)	0.078(1)	0.1628(7)	4.7(3)
C(19)	0.264(1)	-0.302(1)	0.2219(7)	5.2(4)
C(20)	0.2295(9)	-0.172(1)	0.0961(6)	4.7(3)
C(21)	0.0175(9)	0.087(1)	0.3698(8)	4.5(3)
C(22)	0.0934(8)	-0.008(1)	0.4102(7)	3.7(3)
C(23)	0.1642(9)	-0.079(1)	0.3736(7)	3.5(3)
C(24)	0.2695(9)	-0.0595(10)	0.4026(6)	3.4(3)
B(1)	0.2405(9)	0.073(1)	0.2421(7)	2.4(3)

Table 7
Bond distances (Å) of **2**

Ta(1)	C(1)	2.460(9)	C(2)	C(3)	1.40(1)
Ta(1)	C(2)	2.434(9)	C(2)	C(7)	1.51(1)
Ta(1)	C(3)	2.47(1)	C(3)	C(4)	1.42(1)
Ta(1)	C(4)	2.48(1)	C(3)	C(8)	1.50(1)
Ta(1)	C(5)	2.42(1)	C(4)	C(5)	1.41(1)
Ta(1)	C(11)	2.44(1)	C(4)	C(9)	1.49(1)
Ta(1)	C(12)	2.33(1)	C(5)	C(10)	1.50(1)
Ta(1)	C(13)	2.30(1)	C(11)	C(12)	1.42(1)
Ta(1)	C(14)	2.39(1)	C(11)	B(1)	1.54(2)
Ta(1)	C(21)	2.45(1)	C(12)	C(13)	1.38(1)
Ta(1)	C(22)	2.29(1)	C(13)	C(14)	1.43(1)
Ta(1)	C(23)	2.34(1)	C(14)	B(1)	1.54(1)
Ta(1)	C(24)	2.39(1)	C(15)	C(17)	1.52(1)
N(1)	C(15)	1.47(1)	C(15)	C(18)	1.52(1)
N(1)	C(16)	1.47(1)	C(16)	C(19)	1.52(1)
N(1)	B(1)	1.42(1)	C(16)	C(20)	1.51(1)
C(1)	C(2)	1.43(1)	C(21)	C(22)	1.44(2)
C(1)	C(5)	1.42(1)	C(22)	C(23)	1.45(1)
C(1)	9(6)	1.46(1)	C(23)	C(24)	1.42(2)

Table 8
Selected bond angles (°) for **2**

C(15)	N(1)	C(16)	115.5(8)	C(15)	N(1)	B(1)	121.6(8)
C(16)	N(1)	B(1)	121.2(9)	C(21)	C(22)	C(23)	123(1)
C(22)	C(23)	C(24)	120(1)	Ta(1)	C(24)	C(23)	70.6(6)
Ta(1)	C(21)	C(22)	66.4(6)				

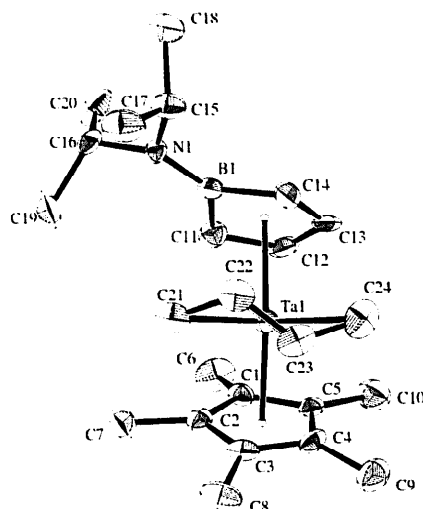
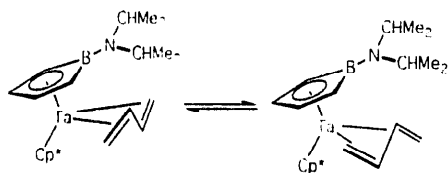


Fig. 2. ORTEP drawing of **2** at 50% probability. Hydrogen atoms are omitted for clarity.

signals remain inequivalent up to 100°C, indicating a minimum activation energy of 18(1) kcal/mol for the automerization exchange:



Analogous degenerate rearrangements in $\text{Cp}_2\text{M}(\text{cis-}\eta^4\text{-butadienes})$ ($\text{M} = \text{Zr}, \text{Hf}$) complexes have activation barriers in the range of 6–15 kcal/mol, depending on metal and substituents on the diene ligand and are believed to proceed via a planar metallacyclopentene transition state [28].

It is also interesting that no evidence exists for $\text{Cp}^*[\text{C}_4\text{H}_4\text{B-N(CHMe}_2)_2]\text{Ta}(\text{cis-}\eta^4\text{-C}_4\text{H}_6)$, even after heating samples of **2** at 100°C for several hours. This tendency of the ' $\text{Cp}^*[\text{C}_4\text{H}_4\text{B-N(CHMe}_2)_2]\text{Ta}$ ' framework for the trans diene is markedly different from ' Cp_2Zr ' and ' Cp_2Hf ' which have a thermodynamic preference for the cis isomer [28].

3. Summary

In summary, two syntheses are described herein which take advantage of cyclopentadienyl mimics to create metallocene-like environments using tantalum. The metal in complex **1** binds more strongly to the carbons in the borabenzene ligand that are furthest from boron. Tantalum is thus electrophilic and prefers to avoid overlap with the electron poor boron. Unlike standard group 4 metallocenes the diene ligand in **2**

binds strongly and prefers a trans stereochemistry. Note that if the borollide ligand is considered as a cis-locked diolefin then **2** contains the two possible diene stereochemistries. The reactivities of both **1** and **2** are under investigation currently and will be reported in due course.

4. Experimental

4.1. General considerations

All manipulations were carried out using either high-vacuum or glovebox techniques as previously described [29]. ^1H and ^{13}C NMR spectra were recorded on a Bruker AMX-400 spectrometer at 400.1 MHz and 100.6 MHz, respectively. Toluene, pentane, diethyl ether and tetrahydrofuran were distilled from benzophenone ketyl. The preparation of $(\text{TBM})\text{TaMe}_2\text{Cl}$ [14], $\text{Cp}^*[\text{C}_4\text{H}_4\text{B-N(CHMe}_2)_2]\text{TaCl}_2$ [19b], $[\text{Li}][\text{Bb-NMe}_2]$ [30] and $\text{Mg}(\text{C}_6\text{H}_6)(\text{THF})_2$ [31] are available in the literature.

4.2. $(\text{TBM})[\text{Bb-NMe}_2]\text{TaMe}_2$ (**1**)

To a tetrahydrofuran (THF) solution of $(\text{TBM})\text{TaMe}_2\text{Cl}$ (0.207 g, 0.391 mmol) was added $[\text{Li}][\text{Bb-NMe}_2]$ (0.045 g, 0.391 mmol) in THF. After stirring for 30 min, the solvent was replaced with toluene (20 ml) and filtered in order to remove the LiCl byproduct. Removal of the toluene affords the product as a dark burgundy oil (0.15 g, 60%). ^1H NMR (C_6D_6): δ 7.26 (d, 6H, *o*-Ph), 7.17 (t, 6H, *m*-Ph), 6.92 (t, 3H, *p*-Ph), 6.48 (ddd, 1H, β -CHCHB, $J_{\text{C-H}} = 1.49, 6.51, 11.35$ Hz), 5.77 (ddd, 1H, β -CH'CHB $J_{\text{C-H}} = 1.49, 6.51, 11.35$ Hz), 5.36 (ddd, 1H, α -CHB, $J_{\text{C-H}} = 1.86, 11.35$ Hz) 5.23 (ddd, 1H, α -CH'B, $J_{\text{C-H}} = 1.86, 11.35$ Hz) 4.92 (t, 1H, γ -CHCHCHB, $J_{\text{C-H}} = 6.51$), 4.44 (bs, 3H, $(\text{PhCH})_3\text{C}^{2-}$), 2.52 (s, 3H, NCH_3), 2.46 (s, 3H, NCH'_3), -0.12 (s, 3H, Ta-CH_3), -0.10 (s, 3H, $\text{Ta-CH}'_3$). ^{13}C NMR (C_6D_6): 142.1 (α -CHB), 136.2, 135.9, 129.5, 125.6 ($\text{PhCH})_3\text{C}^{2-}$), 116.1 (γ -CHCHCHB), 95.9 (β -CHCHB), 50.0 (NCH_3), 44.4 (NCH'_3), 38.4 (Ta-CH_3), 38.3 ($\text{Ta-CH}'_3$). Anal. Calcd for $\text{TaC}_{31}\text{H}_{35}\text{BN}$: C, 60.69; H, 5.76; N, 2.28. Found: C, 60.31; H, 5.41; N, 2.12.

4.3. $\text{Cp}^*[\text{C}_4\text{H}_4\text{B-N(CHMe}_2)_2]\text{Ta}(\eta^4\text{-C}_4\text{H}_6)$ (**2**)

A slight excess of $\text{Mg}(\text{C}_6\text{H}_6) \cdot 2\text{THF}$ (30 mg, 0.14 mmol) suspended in THF was added dropwise to a stirring solution of $\text{Cp}^*[\text{C}_4\text{H}_4\text{B-N(CHMe}_2)_2]\text{TaCl}_2$ (50 mg, 0.091 mmol). An instantaneous color change from green to orange was observed. After stirring for 16 h, the solvent was removed in vacuo and the yellow

product was extracted with pentane. Yield = 67%. Crystalline material precipitated from a concentrated pentane solution at -35°C . ^1H NMR (C_6D_6 , 298K): δ 4.85 (m, 1H, CHCHB), 4.61 (m, 1H, $\text{CH}_2\text{CHCHCH}_2$), 4.36 (m, 1H, CHCHB), 3.34 (sept, 1H, $\text{CH}(\text{CH}_3)_2$), 3.27 (sept, 1H, $\text{CH}(\text{CH}_3)_2$), 2.96 (m, 1H, $\text{CH}_2\text{CHCHCH}_2$), 1.80 (m, 1H, $\text{CH}_2\text{CHCHCH}_2$), 1.73 (m, 1H, CHCHB), 1.55 (m, 1H, $\text{CH}_2\text{CHCHCH}_2$), 1.548 (m, 1H, CHCHB), 1.53 (m, 1H, $\text{CH}_2\text{CHCHCH}_2$), 1.47 (m, 1H, $\text{CH}_2\text{CHCHCH}_2$), 1.43 (d, 3H, $\text{CH}(\text{CH}_3)_2$), 1.41 (s, 15H, C_5Me_5), 1.32 (d, 3H, $\text{CH}(\text{CH}_3)_2$), 1.26 (d, 3H, $\text{CH}(\text{CH}_3)_2$), 1.08 (d, 3H, $\text{CH}(\text{CH}_3)_2$); ^{13}C NMR (C_6D_6) δ 102.6 (C_5Me_5), 90.6 (CHCHB), 88.9 (CHCHB), 85.0 ($\text{CH}_2\text{CHCHCH}_2$), 82.5 ($\text{CH}_2\text{CHCHCH}_2$), 62.3 (CHCHB), 57.7 (CHCHB), 48.9 ($\text{CH}(\text{CH}_3)_2$), 45.0 ($\text{CH}(\text{CH}_3)_2$), 25.0 ($\text{CH}(\text{CH}_3)_2$), 24.4 ($\text{CH}(\text{CH}_3)_2$), 24.1 ($\text{CH}(\text{CH}_3)_2$), 23.5 ($\text{CH}(\text{CH}_3)_2$), 22.7 ($\text{CH}_2\text{CHCHCH}_2$), 14.2 ($\text{CH}_2\text{CHCHCH}_2$), 11.3 (C_5Me_5). Anal. Found: C, 54.00; H, 7.40; N, 2.62. $\text{C}_{24}\text{H}_{39}\text{NBTa}$ Calc.: C, 54.20; H, 7.34; N, 2.63.

Acknowledgements

The authors are grateful to Exxon Chemical Company and the Petroleum Research Fund, administered by the American Chemical Society for financial support.

Tables giving fractional coordinates, thermal parameters and bond distances and angles for **1** and **2** are available. Ordering information is given on any current masthead page.

References

- [1] M. Bochmann, J. Chem. Soc. Dalton Trans. (1996) 255.
- [2] (a) T. Takahashi, M. Hasegawa, N. Suzuki, M. Saburi, C.J. Rousset, P.E. Fanwick, E. Negishi, J. Am. Chem. Soc., 113 (1991) 8564. (b) M.R. Kesti, R.M. Waymouth, Organometallics, 11 (1992) 1095.
- [3] (a) M.R. Gagne, C. Stern, T.J. Marks, J. Am. Chem. Soc., 114 (1992) 275. (b) Y.W. Li, P.-F. Fu, T.J. Marks, Organometallics, 13 (1994) 439.
- [4] (a) J.F. Harrod, Y. Mu, E. Samuel, Polyhedron 10 (1991) 1239. (b) T.D. Tilley, Acc. Chem. Res. 22 (1993) 22, and references therein.
- [5] T. Imori, B. Lu, H. Cal, T.D. Tilley, J. Am. Chem. Soc., 117 (1995) 9931.
- [6] M.F. Hawthorne, Acc. Chem. Res. 1 (1968) 281.
- [7] D.J. Crowther, N.C. Baenziger, R.F. Jordan, J. Am. Chem. Soc., 113 (1991) 1455.
- [8] W.E. Piers, P.J. Shapiro, E.E. Bunel, J.E. Bercaw, Synlettters (1990) 74.
- [9] G.C. Bazan, W.P. Schaefer, J.E. Bercaw, Organometallics 12 (1993) 2126.
- [10] R. Uhrhammer, D.J. Crowther, J.D. Olson, D.C. Swenson, R.F. Jordan, Organometallics 11 (1992) 3098.
- [11] A.K. Saxena, N.S. Hosmane, Chem. Rev. 93 (1993) 1081.
- [12] M.D. Jones, R.D.W. Kemmitt, Adv. Organomet. Chem. 27 (1987) 279.
- [13] G.C. Bazan, G. Rodriguez, B.P. Cleary, J. Am. Chem. Soc., 116 (1994) 2177.
- [14] G. Rodriguez, G.C. Bazan, J. Am. Chem. Soc., 117 (1995) 10155.
- [15] G. Rodriguez, G.C. Bazan, submitted.
- [16] G. Rodriguez, G.C. Bazan, work in progress.
- [17] G.E. Herberich, in: E.W. Abel, F.G.A. Stone, G. Wilkinson (Eds.), Comprehensive Organometallic Chemistry II, vol. 1, Pergamon Press, Oxford, 1995, p. 197.
- [18] R.W. Quan, G.C. Bazan, A.F. Kiely, W.P. Shaeffer, J.E. Bercaw, J. Am. Chem. Soc., 116 (1994) 4489.
- [19] (a) G.C. Bazan, G. Rodriguez, Polyhedron, 14 (1995) 93. (b) G.C. Bazan, S.J. Donnelly, G. Rodriguez, J. Am. Chem. Soc., 117 (1995) 2671.
- [20] G.E. Herberich, U. Englert, M. Hostalek, R. Laven, Chem. Ber., 124 (1991) 17.
- [21] (a) K. Mashima, S. Fujikawa, A. Nakamura, J. Am. Chem. Soc., 117 (1995) 10990. (b) K. Mashima, S. Fujikawa, Y. Tanaka, H. Urata, T. Oshiki, E. Tanaka, A. Nakamura, Organometallics 14 (1995) 2633.
- [22] K. Mashima, S. Fujikawa, H. Urata, E. Tanaka, A. Nakamura, J. Chem. Soc. Chem. Commun. (1994) 1623.
- [23] Ch. Elschenbroich, A. Solzer, Organometallics, VCH, 1992, p. 262.
- [24] G.C. Bazan, G. Rodriguez, A.J. Ashe III, S. Al-Ahmad, C. Müllen, J. Am. Chem. Soc., 118 (1996) 2291.
- [25] G.E. Herberich, H. Ohst, Adv. Organomet. Chem. 25 (1986) 199.
- [26] W.E. Hunter, D.C. Humeir, R.V. Bynum, R.A. Penttila, J.L. Atwood, Organometallics 2 (1983) 750.
- [27] Y. Kal, N. Kanehisa, K. Miki, N. Kasai, K. Mashima, K. Nagasuna, H. Yasuda, A. Nakamura, J. Chem. Soc. Chem. Commun. (1982) 191.
- [28] G. Erker, C. Krueger, G. Mueller, Adv. Organomet. Chem. 24 (1985) 1.
- [29] B.J. Burger, J.E. Bercaw, in: A.L. Wayda, M.Y. Darenbourg (Eds.), Experimental Organometallic Chemistry, ACS Symp. Ser. 357, American Chemical Society, Washington, D.C., 1987.
- [30] (a) A.J. Ashe III, J.W. Kampf, C. Muller, M. Schneider, Organometallics, 15 (1996) 387. (b) A. Qiao, D.A. Hoic, G.C. Fu, J. Am. Chem. Soc., 118 (1996) 6329.
- [31] K. Fujita, Y. Ohnuma, H. Yasuda, H. Tani, J. Organomet. Chem., 113 (1976) 201.